

Cite this: *RSC Adv.*, 2017, **7**, 40881

# Solvent-free and melt aerobic oxidation of benzyl alcohols using $\text{Pd}/\text{Cu}_2(\text{BDC})_2\text{DABCO}$ –MOF prepared by one-step and through reduction by dimethylformamide<sup>†</sup>

Sara Akbari, Javad Mokhtari \* and Zohreh Mirjafari

In this paper we report an efficient method for the aerobic oxidation of benzyl alcohols to aldehydes by supported palladium nanoparticles in a nanoporous metal–organic framework  $\text{Cu}_2(\text{BDC})_2(\text{DABCO})$  ( $\text{BDC} = 1,4\text{-benzenedicarboxylate}$ ,  $\text{DABCO} = 1,4\text{-diazabicyclo[2.2.2]octane}$ ) under a temperature control program and through reduction by dimethylformamide. The  $\text{Pd-NPs}/\text{Cu}_2(\text{BDC})_2(\text{DABCO})$  offered higher catalytic activity and recyclability than reported in literature. The supported Pd nanoparticles ( $\text{PdNPs}/\text{Cu}_2(\text{BDC})_2(\text{DABCO})$ ) were characterized by X-ray diffraction, BET analysis, field emission scanning electron microscopy, transmission electron microscopy, inductively coupled plasma atomic emission spectroscopy and X-ray photoelectron spectroscopy (XPS).

Received 29th June 2017

Accepted 10th August 2017

DOI: 10.1039/c7ra07209k

rsc.li/rsc-advances

The oxidation of organic compounds, such as alcohols is a primary and essential transformation in organic synthesis and industrial chemistry.<sup>1</sup> Among the alcohols, benzyl alcohol is one of the most studied substrates.<sup>2–8</sup> Traditionally, various oxidants, such as peroxides,<sup>9,10</sup> toxic metal oxides,<sup>11</sup> halides,<sup>12</sup> ozone,<sup>13</sup> etc., were used for the oxidation of alcohols. Compared with those oxidants, undoubtedly, air is the most atom-economical and environmentally benign oxidant. Catalysis using metal nanoparticles (MNPs) has attracted great interest in recent years. Considering the current impetus of nanoscience, it is understandable that all aspects related to the preparation of small nanoparticles (NPs) with narrow size distribution, their stabilization and their unique properties compared to large particles.<sup>14–17</sup> The liquid-phase oxidation of alcohols over supported metal catalysts has been extensively studied in the last decade.<sup>18–21</sup> Crystalline microporous and mesoporous metal–organic frameworks (MOFs) are constructed by joining metal-containing units [secondary building units (SBUs)] with organic linkers such as dicarboxylate or other organic rings, using strong bonds (reticular synthesis) to create open crystalline frameworks with permanent porosity.<sup>22</sup> During the past century, extensive work was done on crystalline extended structures in which metal ions are joined by organic linkers containing Lewis base-binding atoms such as nitriles and bipyridines.<sup>23</sup> MOFs have low density, very high surface area with a large percentage of transition metals that can act as

catalytic sites.<sup>24</sup> Also MOFs have a wide range of potential uses including gas storage, separations, solar cells and catalysis.<sup>25</sup> In particular, applications in energy technologies such as fuel cells, supercapacitors, and catalytic conversions have made them objects of extensive study, industrial-scale production, and application.<sup>26</sup> Recently, metal–organic frameworks (MOFs), as a new class of organic inorganic hybrid porous materials, have attracted considerable attention for stabilization and supporting of metal nanoparticles as a novel class of functional materials due to their high surface areas, tunable pore sizes, and thermal stability.<sup>27–29</sup> The employment of MOFs as the supports for PdNPs has attracted considerable interest.<sup>30–32</sup> For catalytic applications, PdNPs have been successfully deposited at the outer surface of the MOF supports ( $\text{Pd}/\text{MOFs}$ )<sup>33–38</sup> or loaded inside the cavities of the MOFs ( $\text{Pd}@\text{MOFs}$ ) *via* various methods such as impregnation and chemical vapor deposition.<sup>39–43</sup> Although great efforts have been made in this field, a general and facile method is needed that can easily introduce the palladium(0) precursor inside the cavities of MOFs in one-pot and without any reducing agent and control the formation of PdNPs with a small particle size, which is beneficial in the cases such as catalysis. Herein, we report the one-step and reducing-agent-free encapsulation of ultrafine PdNPs in to nanopores  $\text{Cu}_2(\text{BDC})_2(\text{DABCO})$  without Pd(0) NPs aggregation on the external surface of framework and application of this catalyst in aerobic oxidation of benzyl alcohols.

$\text{Cu}_2(\text{BDC})_2(\text{DABCO})$  was synthesized and characterized by that are reported in our previous work.<sup>44</sup> At the first we evaluated a simple and straightforward one-step protocol to encapsulate PdNPs inside MOFs through temperature programming control from 80 °C to 130 °C for 20 h.  $\text{Cu}_2(\text{BDC})_2(\text{DABCO})$  has

Department of Chemistry, Science and Research Branch, Islamic Azad University, P.O. Box 14515/775, Tehran, Iran. E-mail: [j.mokhtari@srbiau.ac.ir](mailto:j.mokhtari@srbiau.ac.ir)

† Electronic supplementary information (ESI) available. See DOI: [10.1039/c7ra07209k](https://doi.org/10.1039/c7ra07209k)



been shown to act as a proper support for deposition of PdNPs. Using temperature controlling method after sonication, Pd(II) cations reduced to Pd(0) nanoparticles deposited on the surface of activated  $\text{Cu}_2(\text{BDC})_2(\text{DABCO})$  carriers. The actual loading of Pd(0) was characterized by ICP analysis and found to be 0.9%. To investigate the oxidation state information of palladium, XPS analysis of Pd 3d binding energies was performed. As shown in Fig. 1 the peaks at 341.5 (Pd-3d<sub>3/2</sub>) and 336.2 (Pd-3d<sub>5/2</sub>) eV are due to the binding energy corresponds to the Pd(0), and the peaks at 342.7 (Pd-3d<sub>3/2</sub>) and 337.6 (Pd-3d<sub>5/2</sub>) eV are due to the binding energy corresponds to the Pd(II). Based on the peak areas of Pd-3d<sub>5/2</sub> at 336.2 and 337.6 eV, the ratio of Pd(0) to Pd(II) in Pd/Cu<sub>2</sub>(BDC)<sub>2</sub>DABCO is calculated to be 1.5 (Fig. 1a). XPS analysis of recycling Pd/Cu<sub>2</sub>(BDC)<sub>2</sub>DABCO did not show any significant change in palladium oxidation state (Fig. 1b).

The XRD pattern of PdNPs/Cu<sub>2</sub>(BDC)<sub>2</sub>(DABCO) shows that the crystalline structure of Cu<sub>2</sub>(BDC)<sub>2</sub>(DABCO) is maintained after deposition of PdNPs. The absence of a Pd diffraction pattern relates to the low Pd contents in the materials (Fig. 2).

There have theretofore been many processes reported for the encapsulation of Pd(0) NPs in MOFs but in most of the methods used a reducing agent for reduction of Pd(II) to Pd(0), while in this work we encapsulated and supported Pd(0) NPs in MOFs by temperature control program and without using any reducing agent through reduction by DMF.<sup>45–47</sup> The DMF organic solvent is a powerful reducing agent to reduce different ions such as Ag<sup>+</sup>, Au<sup>3+</sup> and *etc.*<sup>48–50</sup> The possible reaction mechanism for the reduction of Pd<sup>2+</sup> incorporated in MOF by DMF is as the following equation:



This mechanism is supported by a measured increase of conductivity as the reaction proceeds, which indicates that the larger Pd<sup>2+</sup> ions are progressively exchanged for the more mobile H<sup>+</sup> ions. Accordingly, a decrease of the solution pH was observed. Based on a literature report<sup>48–50</sup> we also proposed that carbamic acid produced during the reduction was easily decomposed to dimethyl amine and gaseous CO<sub>2</sub> in high temperature.

Specific surface areas of the samples were measured by N<sub>2</sub> adsorption at 77 K, with results presented in Table 1. Nitrogen adsorption and surface areas of Pd<sup>0</sup>-in-Cu<sub>2</sub>(BDC)<sub>2</sub>(DABCO)

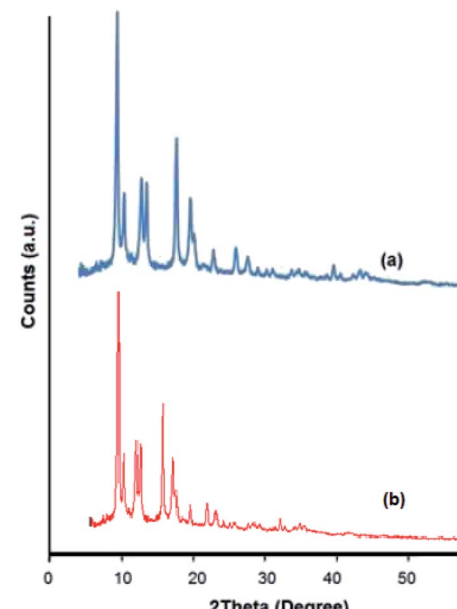


Fig. 2 (a) XRD pattern of prepared Cu<sub>2</sub>(BDC)<sub>2</sub>(DABCO). (b) XRD pattern of prepared PdNPs@Cu<sub>2</sub>(BDC)<sub>2</sub>(DABCO).

Table 1 Textural properties of [Cu<sub>2</sub>(BDC)<sub>2</sub>(DABCO)] and PdNPs@ [Cu<sub>2</sub>(BDC)<sub>2</sub>(DABCO)] from N<sub>2</sub> adsorption–desorption experiments

Material	BET surface area (m <sup>2</sup> g <sup>-1</sup> )	Pore volume (cm <sup>3</sup> g <sup>-1</sup> )
[Cu <sub>2</sub> (BDC) <sub>2</sub> (DABCO)]	1496	0.48
PdNPs@ [Cu <sub>2</sub> (BDC) <sub>2</sub> (DABCO)]	873	0.475

samples were noticeably reduced compared to Cu<sub>2</sub>(BDC)<sub>2</sub>(DABCO), indicating that the cavities of Cu<sub>2</sub>(BDC)<sub>2</sub>(DABCO) may be occupied by highly dispersed Pd nanoparticles (Table 1).

TEM micrograph (Fig. 3), confirmed that a crystalline and nano-scaled material was produced. It is also to emphasize that Pd nanoparticle has resulted in producing uniformly distributed nano-scale. It is also to emphasize that Pd nanoparticle has resulted in producing uniformly distributed nano-scale and with a mean particle diameter of  $2.9 \pm 0.2$  nm as estimated from particle size distribution.

The synthetic PdNPs/Cu<sub>2</sub>(BDC)<sub>2</sub>DABCO was employed as a catalyst in the aerobic oxidation of benzyl alcohols (Scheme 1).

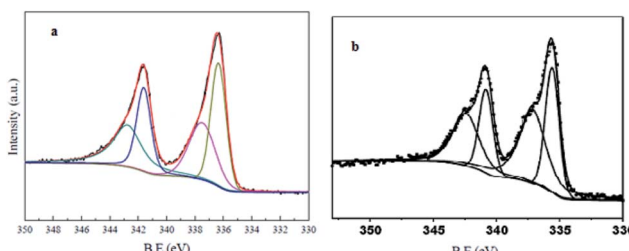


Fig. 1 (a) XPS spectrum of synthesized Pd-NPs/Cu<sub>2</sub>(BDC)<sub>2</sub>DABCO and (b) recycled Pd-NPs/Cu<sub>2</sub>(BDC)<sub>2</sub>DABCO.

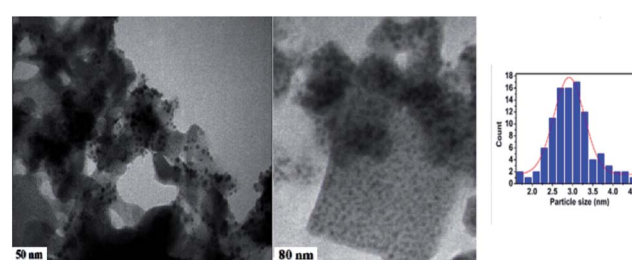
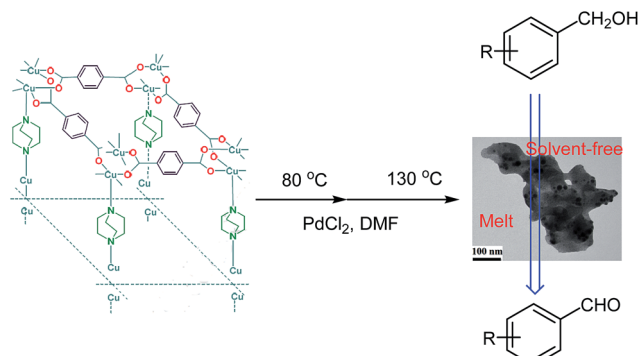


Fig. 3 TEM micrograph of the PdNPs/Cu<sub>2</sub>(BDC)<sub>2</sub>DABCO.



**Scheme 1** Schematic representation of PdNPs@Cu<sub>2</sub>(BDC)<sub>2</sub>DABCO catalyzed oxidation of benzyl alcohols.

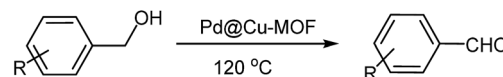
Benzyl alcohol was chosen as a model substrate to study the catalytic activity of PdNPs/Cu<sub>2</sub>(BDC)<sub>2</sub>DABCO to identify suitable reaction conditions using atmospheric air as the terminal oxidant. The results are presented in Table 1. Initially, the oxidation of benzyl alcohol was tested in CH<sub>3</sub>CN at 80 °C with 20 mg of PdNPs/Cu<sub>2</sub>(BDC)<sub>2</sub>DABCO (0.9% Pd) and a stream of air produced by air pump was conducted into the reaction mixture, in this condition negligible yield of benzaldehyde was attained. When oxidation of benzyl alcohol was tested in toluene at 110 °C, conversion of benzyl alcohol to the benzaldehyde was increased. These tests shown that the nature of solvent and temperature greatly affect the efficiency of oxidation. So, in another attempts for confirmation of this hypothesis, reaction was performed in xylene at 135 °C. As expected, conversion of benzyl alcohol was increased. From the viewpoint of green chemistry and toxicity of above solvent, in another attempt, when oxidation of benzyl alcohols was performed in absences of solvent and under solvent-free condition at 120 °C, conversion increased significantly.

In another attempt to investigate the role of the base in the rate and yield of oxidation, a catalytic amount of mineral base

(20 mol% Na<sub>2</sub>CO<sub>3</sub> or K<sub>2</sub>CO<sub>3</sub>) was used. As was expected the rates and yields improved.

For the optimization of loading of the catalyst, different amount of catalyst was used. As shown in Table 2, with increasing the amount of catalyst, yield was improved (Table 2, entry 5–7). In another attempt, when the reaction was carried out in the absence of PdNPs/Cu<sub>2</sub>(BDC)<sub>2</sub>DABCO or Cu<sub>2</sub>(BDC)<sub>2</sub>DABCO, no product was formed after 24 hours at 120 °C. It has been observed that PdNPs/Cu<sub>2</sub>(BDC)<sub>2</sub>DABCO promotes the oxidation of benzyl alcohol under solvent-free condition with

**Table 3** Oxidation of different benzyl alcohols



Entry	R	Time (h)	Yield <sup>a</sup>
1	H	24	99
2	4-Me	24	97
3	2-Me	24	96
4	4-OMe	24	93
5	4-Cl	24	96
6	4-Br	24	95
7	4-NO <sub>2</sub>	24	96
8	2-NO <sub>2</sub>	24	97

<sup>a</sup> Isolated yield.

**Table 4** Reusability test of catalyst

Experiment no.	Yield
1	98
2	95
3	95
4	93

**Table 2** Optimization of reaction conditions



Run	Catalyst (mg)	Solvent	Base (20 mol%)	Time (h)	T (°C)	Yield <sup>a</sup> (%)
1	15	CH <sub>3</sub> CN	Na <sub>2</sub> CO <sub>3</sub>	24	80	5
2	15	Toluene	Na <sub>2</sub> CO <sub>3</sub>	24	110	20
3	15	Xylene	Na <sub>2</sub> CO <sub>3</sub>	24	135	40
4	15	—	Na <sub>2</sub> CO <sub>3</sub>	24	120	89
5	<b>20</b>	—	<b>Na<sub>2</sub>CO<sub>3</sub></b>	<b>24</b>	<b>120</b>	<b>99</b>
6	25	—	Na <sub>2</sub> CO <sub>3</sub>	24	120	90
7	30	—	Na <sub>2</sub> CO <sub>3</sub>	24	120	95
8	—	—	Na <sub>2</sub> CO <sub>3</sub>	24	120	0
9	20	—	—	24	120	51
10	Cu-MOF (20 mg)	—	Na <sub>2</sub> CO <sub>3</sub>	24	120	15

<sup>a</sup> Isolated yield.



Table 5 Comparison of activity for different catalytic systems in the oxidation of benzyl alcohols

Entry	Catalyst	Reaction condition	Yield	(Sel.%)	Ref. no.
1	Pd@C-GluA-550	Substrate 4 mL/air 1 atm/120 °C	48.9	63	53
2	Pd@C-GluA-550	Solvent-free/O <sub>2</sub> (1 MPa)/120 °C	48.9	80	53
3	Pd/NaX zeolite	Toluene/100 °C/O <sub>2</sub> (3 mL min <sup>-1</sup> )	66	97	54
4	Pd/Al <sub>2</sub> O <sub>3</sub>	Solvent free/120 °C/O <sub>2</sub> (50 mL min <sup>-1</sup> )	80	94	55
5	Pd cluster colloid	Water/32 °C/air bubbling/(pH 3.5)	86	100	56
6	MNP-Pd	Toluene/K <sub>2</sub> CO <sub>3</sub> /85–90 °C/air	89	93	57
7	Pd@Cu <sub>2</sub> (BDC) <sub>2</sub> DABCO	Solvent free/Na <sub>2</sub> CO <sub>3</sub> (20 mol%)/air	99	100	Present work

atmospheric air. So, as shown in Table 2 the best result observed in entry 5.

For review of the catalytic performance of Cu<sub>2</sub>(BDC)<sub>2</sub> (DABCO) on the aerobic oxidation of benzyl alcohol an experiment was performed as shown in Table 2 entry 10. As expected, little efficiency was achieved. It can be concluded that palladium is very effective in this study.

Encouraged by this success, we next investigated the scope of the oxidation of benzyl alcohols derivatives (Table 3). The aerobic oxidation reactions of the benzylic alcohols with different substituted groups under solvent-free were carried out in air (monitored by GC).

We found that all benzylic alcohols with both electron-withdrawing (–NO<sub>2</sub>) and electron-donating groups (–OMe, –Me) at either *para*- or *ortho*-position gave excellent conversions. To determine the degree of leaching of the palladium from the PdNPs/Cu<sub>2</sub>(BDC)<sub>2</sub>DABCO catalyst, after the filtration of catalyst the palladium content of the filtrate was determined by ICP. It was shown that less than 0.1% of the total amount of the original palladium species was lost into solution during the reaction. This leaching level was negligible which was also confirmed by the excellent reusability of this heterogeneous catalyst.

One of the important properties of the heterogeneous catalyst is the reusability, so to confirm this for our catalyst, we performed recycling experiment; so the oxidation of benzyl alcohol was chosen as a model reaction with recycled catalyst;

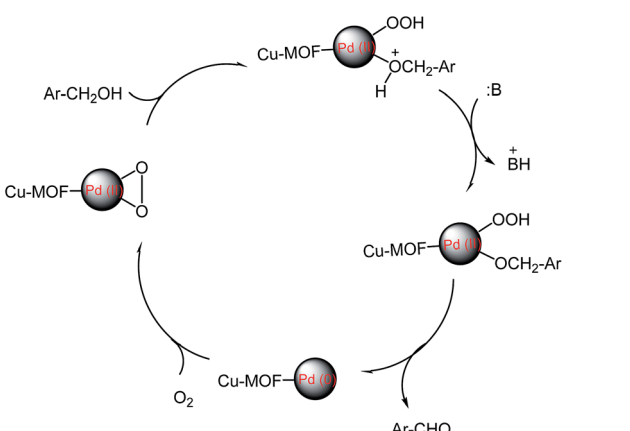
the reaction was completed after 24 hour and the conversion and isolated yield of the reaction was 100 and 98%, respectively (experimental section). This reusability test was repeated for three times and the result summarized in Table 4.

A comparison with other catalytic systems in the oxidation of benzyl alcohol demonstrated that our present Pd/MOF catalyst system exhibited a higher conversion and yield under milder conditions (Table 5). In the literature has been reported that the oxidative dehydrogenation of alcohols to the corresponding aldehydes happened on all exposed metallic palladium faces and the undesired products such as toluene, benzyl ether often produce on hollow sites of Pd particle faces.<sup>51</sup> However, in our work, undesired products not were formed, so we proposed that the sites on face centered cubic Pd are the primary sites for the oxidation of benzyl alcohols.<sup>52</sup> The proposed mechanism for this reaction is given below (Scheme 2).

The structures of all products were elucidated from their melting point (for the solid product) and <sup>1</sup>H-NMR spectra.

## Materials and instruments

All reagents including organic linker H<sub>2</sub>BDC, metal salt Cu(OAc)<sub>2</sub>·H<sub>2</sub>O, 1,4-benzenedicarboxylate (BDC, 99%), 1,4-diazabicyclo[2.2.2]octane (DABCO), palladium(II) chloride (PdCl<sub>2</sub>), benzyl alcohols and solvent were obtained from commercially available sources such as Sigma-Aldrich and Merck without any purification. X-ray powder diffraction (XRD) measurements were performed using an Xpert MPD. Philips diffractometer with Cu radiation source ( $\lambda = 1.54050 \text{ \AA}$ ) at 40 kV voltage and 40 mA current. BET (Brunauer-Emmett-Teller) surface area of the samples was determined from N<sub>2</sub> adsorption-desorption isotherms using a micromeritics ASAP 2020 analyzer. The sample was characterized using a scanning electron microscope (SEM) with a ZEISS at 30 kV with gold coating. Transmission electron microscopy (TEM) was carried out using an EM10C-100 kV series microscope from the Zeiss Company, Germany. The actual loading of palladium was determined by Inductively Coupled Plasma (ICP) analysis on sequential plasma spectrometer, Shimadzu (ICPS-7000 ver. 2). X-ray photoelectron spectroscopy (XPS) measurements were conducted on a PHI Quantum 2000 XPS system equipped with an Al X-ray source (1486.6 eV). <sup>1</sup>H-NMR spectra were measured (CDCl<sub>3</sub>) with a Bruker DRX-500 AVANCE spectrometer at 400.13. Melting points were measured on an Electrothermal 9100 apparatus and



Scheme 2 Proposed mechanism for the oxidation of benzyl alcohols.



GC analysis of determination of conversions and selectivities was performed on an Agilent 6890N.

## One-step supporting of palladium nanoparticle in $\text{Cu}_2(\text{BDC})_2(\text{DABCO})$ ( $\text{Pd}/\text{Cu}_2(\text{BDC})_2(\text{DABCO})$ )

$[\text{Cu}_2(\text{BDC})_2\text{DABCO}]$  was synthesized by that are reported in our previous work.<sup>40</sup> A mixture of  $\text{Cu}(\text{OAc})_2 \cdot \text{H}_2\text{O}$  (0.6 mmol),  $\text{H}_2\text{BDC}$  (0.6 mmol) and DABCO (0.3 mmol) with molar ratio of 2 : 2 : 1 were ball-milled vigorously at 28 Hz at room temperature for 2 hours. The obtained green powder was washed with DMF ( $3 \times 10$  mL). Solvent exchange was carried out with methanol ( $3 \times 10$  mL) at room temperature. To remove the guest molecules of MOFs, obtained powder was treated by heating under vacuum at  $130^\circ\text{C}$  for 12 hours, resulting in 1.6 g of pure product which corresponds to 94% isolated yield.

The synthesized  $\text{Cu}_2(\text{BDC})_2(\text{DABCO})$  (0.1 g) was dissolved in 2 mL of DMF and then 3 mg of  $\text{PdCl}_2$  with purity of 99.9% were added to the mixture. The solution was sonicated for 20 min, then stirred at  $80^\circ\text{C}$  for 20 h and finally it was stirred at  $130^\circ\text{C}$  with the purpose of reduction of  $\text{Pd}(\text{II})$  to  $\text{Pd}(\text{0})$  and encapsulation in cavities of MOF. Finally, the product  $\text{PdNPs}/\text{Cu}_2(\text{BDC})_2(\text{DABCO})$  was centrifuged, washed with DMF and methanol and dried in vacuum at  $120^\circ\text{C}$  for 12 h.

## Catalyst usage for the oxidation of benzyl alcohols

In a typical oxidation, 0.5 mL substrate (grams for the solid benzyl alcohols), catalysts and base used as described in the manuscript and were added into a 10 mL three-neck round-bottom flask, which was fitted with a magnetic stirrer and an air inlet tube. The reaction was performed at  $120^\circ\text{C}$  in an oil bath with magnetic stirring. A stream of air produced by air pump was conducted into the reaction mixture and controlled by a flow meter at a constant flow rate ( $5 \text{ mL min}^{-1}$ ). After completion of the reaction that monitored by TLC, ethyl acetate was added to the reaction mixture and catalyst was filtered. The filtrate was analysed by GC. The solvent was evaporated on a rotary evaporator to afford benzaldehyde (0.5 g, 98%) which in some cases were essentially pure cyanohydrin TMS ethers. All of the aldehydes characterized by melting point (for solids) and  $^1\text{H-NMR}$  spectroscopy and confirmed with what is reported in the literature.<sup>48-52</sup>

In the reusability test, oxidation of benzyl alcohol under above condition was chosen as a model reaction, the conversion and isolated yield was 100 and 91% respectively.

## Conclusions

In summary, we have successfully developed a facile and effective strategy to prepare PdNPs supported on  $\text{Cu}_2(\text{BDC})_2$  (DABCO) and on-site moderate reduction process to control the size and location of PdNPs within MOFs. This synthesis process could be achieved in one step through a simple temperature

control program without adding any external reduction agent. The Pd/MOFs offered higher catalytic activity than common palladium salts for the quantitative and selective oxidation of benzyl alcohols. Further studies on encapsulation of other useful PdNPs in MOFs and development of its catalytic scope are in progress and would be presented in due course.

## Conflicts of interest

There are no conflicts to declare.

## Acknowledgements

The authors gratefully acknowledge from Science and Research Branch, Islamic Azad University for partial financial support of this work.

## References

- 1 R. A. Sheldon and J. K. Kochi, *Metal-Catalyzed Oxidations of Organic Compounds*, Academic Press, 1981.
- 2 M. Saiman, *Angew. Chem., Int. Ed.*, 2012, **51**, 5981–5985.
- 3 X. Tong, J. Xu and H. Miao, *Adv. Synth. Catal.*, 2005, **347**, 1953–1957.
- 4 S. S. Shannon, *Science*, 2005, **309**, 1824–1826.
- 5 K. P. Peterson and R. C. Larock, *J. Org. Chem.*, 1998, **63**, 3185–3189.
- 6 M. J. Schultz, C. C. Park and M. S. Sigman, *Chem. Commun.*, 2002, 3034–3035.
- 7 T. Iwasawa, M. Tokunaga, Y. Obora and Y. Tsuji, *J. Am. Chem. Soc.*, 2004, **126**, 6554–6555.
- 8 S. S. Shannon, *Angew. Chem., Int. Ed.*, 2004, **43**, 3400–3420.
- 9 Y. Wang, J. S. Zhang, X. C. Wang, M. Antonietti and H. R. Li, *Angew. Chem., Int. Ed.*, 2010, **49**, 3356–3359.
- 10 H. Zhou, *Chem. Commun.*, 2012, **48**, 6954–6956.
- 11 J. Muzart, *Chem. Rev.*, 1992, **92**, 113–140.
- 12 X. Tong, J. Xu and H. Miao, *Adv. Synth. Catal.*, 2005, **347**, 1953–1957.
- 13 M. Waser, W. G. Jary, P. Pochlauer and H. Falk, *J. Mol. Catal. A: Chem.*, 2005, **236**, 187–193.
- 14 Y. Huang, Z. Zheng, T. Liu, J. Lu, Z. Lin, H. Li and R. Cao, *Catal. Commun.*, 2011, **14**, 27.
- 15 A. S. Roy, J. Mondal, B. Banerjee, P. Mondala and A. Bhaumik, *Appl. Catal., A*, 2014, **469**, 320.
- 16 P. Puthiaraj and W. S. Ahn, *Catal. Commun.*, 2015, **65**, 91.
- 17 S. Gao, N. Zhao, M. Shu and S. Che, *Appl. Catal., A*, 2010, **338**, 196.
- 18 M. Besson and P. Gallezot, *Catal. Today*, 2000, **57**, 127–141.
- 19 T. Mallat and A. Baiker, *Chem. Rev.*, 2004, **104**, 3037–3058.
- 20 N. Dimitratos, J. A. Lopez-Sanchez and G. J. Hutchings, *Chem. Sci.*, 2012, **3**, 20–44.
- 21 S. E. Davis, M. S. Ide and R. J. Davis, *Green Chem.*, 2013, **15**, 17–45.
- 22 O. M. Yaghi, *Nature*, 2003, **423**, 705.
- 23 (a) A. F. Wells, *Structural Inorganic Chemistry*, Oxford Univ. Press, New York, 1984; (b) Y. Kinoshita, I. Matsubara, T. Higuchi and Y. Saito, *Bull. Chem. Soc. Jpn.*, 1959, **32**, 1221.

24 (a) D. J. Tranchemontagne, J. L. Mendoza-Cortés and M. O'Keeffe, *Chem. Soc. Rev.*, 2009, **38**, 1257; (b) M. Ranocchiari and J. A. VanBokhoven, *Phys. Chem. Chem. Phys.*, 2011, **13**, 6388; (c) U. Mueller, *J. Mater. Chem.*, 2006, **16**, 626.

25 (a) M. Jacoby, *Chem. Eng. News*, 2008, **86**, 13; (b) S. H. Hsu, C. T. Li, H. T. Chien, R. R. Salunkhe, N. Suzuki, Y. Yamauchi, K. C. Ho and K. C. W. Wu, *Sci. Rep.*, 2014, **4**, 6983; (c) Y. C. Sue, J. W. Wu, S. E. Chung, C. H. Kang, K. Tung, K. C. Wu and F. K. Shieh, *ACS Appl. Mater. Interfaces*, 2014, **6**, 5192–5198; (d) F. K. Shieh, S. C. Wang, C. Yen, C. Wu, S. Dutta, L. Y. Chou, J. V. Morabito, P. Hu, M. H. Hsu, K. C. W. Wu and C. K. Tsung, *J. Am. Chem. Soc.*, 2015, **137**, 4276–4279.

26 M. Meilikov, K. Yusenko, D. Esken, S. Turner, G. Van Tendeloo and R. A. Fischer, *Eur. J. Inorg. Chem.*, 2010, 3701–3714.

27 H. Kobayashi, Y. Mitsuka and H. Kitagawa, *Inorg. Chem.*, 2016, **55**, 7301–7310.

28 P. Falcaro, R. Ricco, A. Yazdi, I. Imaz, S. Furukawa, D. MasPOCH, R. Ameloot, J. D. Evans and C. J. Doonan, *Coord. Chem. Rev.*, 2016, **307**, 237–254.

29 A. S. Roy, J. Mondal, B. Banerjee, P. Mondala and A. Bhaumik, *Appl. Catal., A*, 2014, **469**, 320.

30 P. Puthiaraj and W. S. Ahn, *Catal. Commun.*, 2015, **65**, 91.

31 S. Gao, N. Zhao, M. Shu and S. Che, *Appl. Catal., A*, 2010, **388**, 196.

32 B. Yuan, Y. Pan, Y. Li, B. Yin and H. Jiang, *Angew Chem., Int. Ed.*, 2010, **49**, 4054.

33 L. Zhang, Z. Su, F. Jiang, Y. Zhou, W. Xu and M. Hong, *Tetrahedron*, 2013, **69**, 9237.

34 N. Shang, S. Gao, X. Zhou, C. Feng, Z. Wang and C. Wang, *RSC Adv.*, 2014, **4**, 54487.

35 V. Pascanu, Q. Yao, A. Bermejo Gomez, M. Gustafsson, Y. Yun, W. Wan, L. Samain, X. Zou and B. Martin-Matute, *Chem.-Eur. J.*, 2013, **19**, 17483.

36 L. Shen, W. Wu, R. Liang, R. Lin and L. Wu, *Nanoscale*, 2013, **5**, 9374.

37 J. Juan-Alcaniz, J. Ferrando-Sori, I. Luz, P. Serra-Crespo, E. Skupien, V. P. Santos, E. Pardo, I. Llabres, F. X. Xamena, F. Kapteijn and J. Gascon, *J. Catal.*, 2013, **307**, 295.

38 V. Pascanu, P. R. Hansen, A. Bermejo Gomez, C. Ayats, A. E. Platero-Prats, M. J. Johansson, M. A. Pericas and B. Martin-Matute, *ChemSusChem*, 2015, **8**, 123.

39 Y. Huang, S. Liu, Z. Lin, W. Li, X. Li and R. Cao, *J. Catal.*, 2012, **292**, 111.

40 M. Zhang, J. Guan, B. Zhang, D. Su, C. T. Williams and C. Liang, *Catal. Lett.*, 2012, **142**, 313.

41 N. T. S. Phan, T. T. Nguyen and L. Vu, *ChemCatChem*, 2013, **5**, 3068.

42 M. Klimakow, P. Klobes, K. Rademann and F. Emmerling, *Microporous Mesoporous Mater.*, 2012, **154**, 113.

43 A. Pichon, A. Lazuen-Garay and S. L. James, *CrystEngComm*, 2006, **8**, 211.

44 L. Panahi, M. R. Naimi-Jamal, J. Mokhtari and A. Morsali, *Microporous Mesoporous Mater.*, 2017, **244**, 208.

45 L. Chen, X. Chen, H. Liu, C. Baia and Y. Li, *J. Mater. Chem. A*, 2015, **3**, 15259.

46 J. Y. Yu, S. Schreiner and L. Vaska, *Inorg. Chim. Acta*, 1990, **170**, 145.

47 (a) Z. A. Qiao, P. F. Zhang, S. H. Chai, M. F. Chi, G. M. Veith, N. C. Gallego, M. Kidder and S. Dai, *J. Am. Chem. Soc.*, 2014, **136**, 11260–11263; (b) S. Rana, S. Maddila and S. B. Jonnalagadda, *Catal. Sci. Technol.*, 2015, **5**, 3235–3241.

48 I. P. Santos and L. M. L. Marzan, *Nano Lett.*, 2002, **2**, 903.

49 I. P. Santos and L. M. L. Marzan, *Adv. Funct. Mater.*, 2009, **19**, 679.

50 I. P. Santos and L. M. L. Marzan, *Langmuir*, 1999, **15**, 948.

51 Z. A. Qiao, P. F. Zhang, S. H. Chai, M. F. Chi, G. M. Veith, N. C. Gallego, M. Kidder and S. J. Dai, *J. Am. Chem. Soc.*, 2014, **136**, 11260–11263.

52 K. Mori, T. Hara, T. Mizugaki, K. Ebitani and K. Kaneda, *J. Am. Chem. Soc.*, 2004, **126**, 10657–10666.

53 P. Zhang, Y. Gong, H. Li, Z. Chen and Y. Wang, *Nat. Commun.*, 2013, **4**, 1593.

54 F. Li, Q. H. Zhang and Y. Wang, *Appl. Catal., A*, 2008, **334**, 217–226.

55 X. M. Wang, G. J. Wu, N. J. Guan and L. D. Li, *Appl. Catal., B*, 2012, **115**, 7–15.

56 R. R. Dun, X. G. Wang, M. W. Tan, Z. Huang, X. M. Huang, W. Z. Ding and X. G. Lu, *ACS Catal.*, 2013, **3**, 3063–3066.

57 D. Wang, C. Deraedt, L. Salmon, C. Labrugère, L. Etienne, J. Ruiz and D. Astruc, *Chem.-Eur. J.*, 2015, **21**, 6501–6510.